Evidence for a general mechanism modulating carrier lifetime in SiC

Bin Chen,[1,*] Takashi Sekiguchi,[1] Takasumi Ohyanagi,[2] Hirofumi Matsuhata,[2] Akimasa Kinoshita,[2] and Hajime Okumura[2]
[1]*National Institute for Materials Science, Tsukuba 305-0044, Japan*
[2]*National Institute of Advanced Industrial Science and Technology, Tsukuba 305-8568, Japan*
(Received 6 April 2010; revised manuscript received 28 May 2010; published 23 June 2010)

Stacking faults (SFs) in semiconductors are generally regarded as the electrically active defects that reduce the minority carrier lifetime. In contrast to this typical phenomenon, here we report that the SFs in SiC functionalize as the ideal quantum well (QW) structure for electrons. Due to the QW effect, an increase of minority carrier lifetime is observed at the SF regions. The reason for the lifetime increment is discussed with the electron dissipation along the SF plane. Our results suggest that this is a general mechanism regarding the increase of minority carrier lifetime at the defects.

DOI: 10.1103/PhysRevB.81.233203 PACS number(s): 73.21.Fg, 61.72.Nn, 73.63.Hs, 73.50.Gr

Stacking faults (SFs) are one of the most fundamental planar defects in crystalline solids. The SFs occur in a number of crystal structures, but the common example is in close-packed structures. In Si material, the SFs are usually formed on {111} planes by the application of a shear stress and are regarded as the electrically active defects.[1,2] In a compound semiconductor, such as SiC, the situation becomes complicated since SiC is known to have hundreds of different polytypes.[3–5] Especially, the polymorphism of SiC is particular in that all its different crystalline forms have a same atomic plane in common and differ only in the stacking sequence along the direction normal to this plane. It has been reported that SiC has a very low SF energy.[6] Therefore, various kinds of SFs are expected to appear if the local stacking sequence is interrupted somewhat with respect to the host material.

Indeed, several types of SFs differing in the stacking arrangement have been already observed in SiC.[7–11] Since SiC is a promising wide-bandgap semiconductor aimed at high-power, high-frequency, and high-temperature applications, many investigations of the SFs are related to the devices (*p-i-n* diodes), such as the following aspects: (i) the degradation of SiC devices;[12,13] (ii) the nucleation sites of the SFs;[14–16] (iii) the driving force for the SF expansion under forward bias stressing;[17–19] (iv) partial dislocations (PDs) bounding the SFs[20–22] and (v) theoretical calculation of the electronic state of the SFs.[23–25] However, the fundamental/intrinsic properties of the SFs in SiC have not been clarified very well. The clarification may provide fundamental knowledge of SF behavior in polytypic materials as well as further facilitate the understanding of SF effect on device properties.

In this paper, we report on the intrinsic feature of the SFs in SiC. Different from the common feature in Si, we show that the SFs in SiC act as the ideal quantum-well (QW) structure for electrons. We also observe an increase of minority carrier lifetime at the SFs, which is not generally expected. We thus propose that the lifetime increment is associated with the QW-related "pump effect" dissipating the majority carriers, which would be a general mechanism regarding the increase of minority carrier lifetime at the defects.

The common polytype of SiC, 4H, was used in this work. The 4H-SiC epi-films (6 μm thick) were grown on the n^+-type 4H-SiC (0001) off-cut substrate oriented 8° toward the $\langle 11\bar{2}0\rangle$ direction by chemical vapor deposition. The epitaxial films were N doping, with the concentration of $\sim 1.8\times 10^{16}$ cm^{-3}. For electrical characterization, the Schottky (ITO, 100 nm) and Ohmic contacts (Ni, 200 nm) were formed on the film surfaces and the backside of the substrates, respectively.

The carrier dynamics related the SFs were investigated by using the cathodoluminescence (CL) and electron-beam-induced current (EBIC) techniques. These two systems are integrated in a scanning electron microscope (SEM, S4200-SE). The beam voltage and beam current used for the characterization were 20 kV and 3 nA, respectively. The observation temperatures were varied from 100 K to room temperature (RT) using the specimen cooling system flowing liquid helium gas.[26] The EBIC contrast that reflects the electrical activity of a defect is defined by,

$$C_{EBIC} = \frac{I_{BG} - I_D}{I_{BG}} \times 100 \quad (\%)$$

where I_{BG} and I_D are the EBIC currents at the background (BG) and at the defect, respectively. The transmission electron microscopy (TEM) samples of the SFs were prepared by focused ion beam, and the structures of the SFs were observed by using high-resolution TEM (JEM-2100F).

Figure 1 shows the EBIC monitoring of the formation of a SF at RT. In the EBIC images, defects are generally seen as dark features due to the carrier recombination. At the beginning, a dark line and two dark dots were observed in Fig. 1(a). The dark line corresponds to a basal plane dislocation (BPD) located in the (0001) plane, which has the Burgers vector of $1/3\langle 11\bar{2}0\rangle$ identified by x-ray topography.[27] The BPD intersects the sample surface at the right end. The dark dots are related to threading dislocations (TDs) lying almost perpendicular to the sample surface.

After the electron beam (e-beam) irradiation for 20 min, the BPD dissociates into a partial dislocation loop (PDL), with the formation of a SF inside [Fig. 1(b)]. We notice that one PD nearly stays at the same position as the initial BPD, while the other one moves, resulting in the subsequent expansion of the SF. Generally, two kinds of partials exist in SiC: either the core contains Si atoms or C atoms. These two partials are expected to present different mobilities, because the bonds constituting the two types of cores are chemically

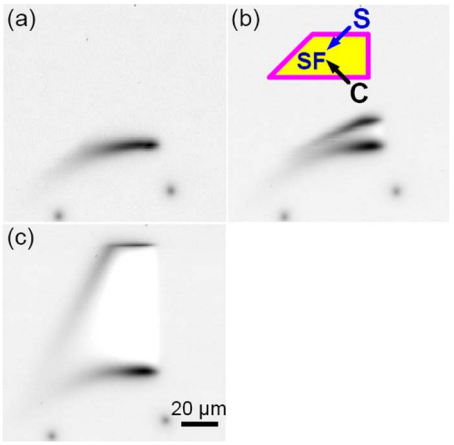

FIG. 1. (Color online) EBIC monitoring the formation of a SF through engineering a BPD. (a) Initial stage of the observation. The dark line corresponds to a BPD, while the dark dots are related to TDs. (b) Electron-beam irradiation for 20 min. The BPD dissociates into a PDL, with a SF formed inside. The schematic is shown in the inset. (c) Electron-beam irradiation for 80 min. The leading PD continues to move upwards, resulting in the expansion of the SF.

distinct. It has been reported that the trailing PD has a C core (marked C), while the leading one has a Si core (marked S).[21,22] The schematic is illustrated inside Fig. 1(b). The SF continues to expand during the e-beam irradiation, e.g., when irradiated for 80 min, a large SF of ~80 μm was achieved [Fig. 1(c)]. It is worth noting that the SF region is bright in the EBIC images, which will be discussed later.

The fabricated SFs act as the QW structure for electrons, which is recognized by the CL characterization. Figure 2(a) presents the RT CL spectra taken at the BG and the SF region. At the BG, a peak at 3.22 eV (wavelength of 385 nm) was resolved, which corresponds to the band-edge emission of 4H-SiC. In contrast to the BG, a new peak at 2.97 eV (wavelength of 417 nm) appears at the SF. In the CL mapping at 417 nm [inset of Fig. 2(a)], the trapezoid region with the high CL intensity corresponds to the SF, which indicates that the 417 nm emission originates from the SF. It is noticed that the energy difference between the band-edge emission and the SF is 0.25 eV, which introduces a QW state. The QW level is 0.25 eV lower with respect to the conduction band minimum of 4H-SiC by comparing with the theoretical calculations.[23] Through this QW state, the SF can effectively capture the electrons from the conduction band, and thus emit the characteristic CL.

We further performed the low-temperature CL observation to understand the SF-related QW, as shown in Fig. 2(b). The CL intensity of the SF peak is the maximum at 100 K, and then decreases with increasing the temperatures. The temperature dependence of CL intensity was considered by taking into account of Fermi level position. The Fermi level is nearly pinned at the N donor level [0.06~0.09 eV (Ref. 28)] at 100 K, while it approaches to the bottom of the QW at RT. As a result, the occupancy of electrons inside the QW is reduced by increasing the temperatures. The luminescence through the carrier recombination involving the SF level and the 4H-SiC valence band edge then becomes weaker as the temperature increases.

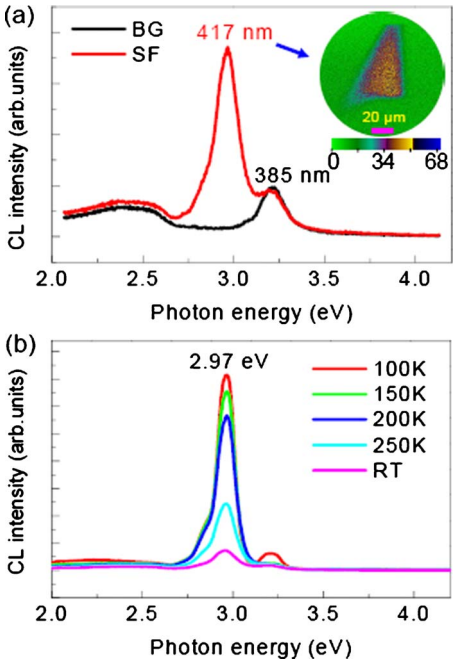

FIG. 2. (Color online) CL spectra taken at the BG and the SF regions. (a) RT CL spectra. The 385 nm (3.22 eV) emission corresponds to the band-edge emission of 4H-SiC, while a new peak at 2.97 eV (wavelength of 417 nm) is related to the SF. The inset shows the CL mapping image at 2.97 eV. (b) Temperature-dependent CL spectra of the SF from 100 K to RT. The CL intensity of the SF-related peak decreases by increasing the temperatures.

To check whether the SF-related QW is ideal, the structure of the SFs was investigated by TEM. Figure 3(a) shows the high-resolution TEM micrograph of a SF. The micrograph was viewed along the $[11\bar{2}0]$ zone axis of the 4H crystal. In the classical *ABC* notation of the layer stacking, 4H structure has an ordering sequence *ABCB* of the planes, where each plane corresponds to a Si-C bilayer. The perfect 4H stacking is guided by the yellow dotted lines. Between the 4H structure, the ordering sequence (marked by a red dotted line) changes somewhat with respect to the host 4H.

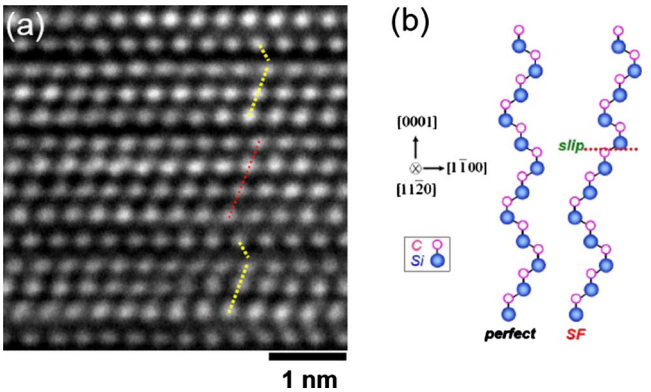

FIG. 3. (Color online) Structure and schematic formation of the SF viewed along the $[11\bar{2}0]$ zone axis. (a) High-resolution TEM observation of the SF. The perfect 4H is guided by the yellow dotted lines, while the SF region is marked by the red straight dotted line. (b) Schematic illustrating the formation of the SF.

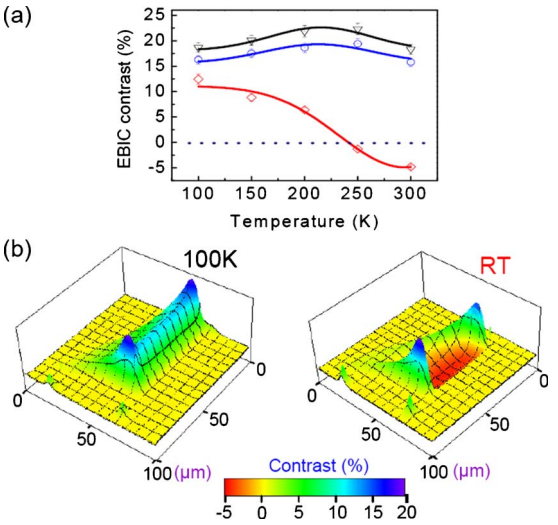

FIG. 4. (Color online) Temperature-dependent EBIC contrasts and profiles of the SF and PDs. (a) The EBIC contrast of the SF (red rectangle) gradually decreases as the temperature increases, and changes to negative after ~250 K. The EBIC contrasts of C (black triangle) and S (blue circle) PDs increases with increasing the temperature, and then decrease a little after ~250 K. (b) Three-dimensional EBIC contrast profiles of the SF at 100 K and RT, respectively.

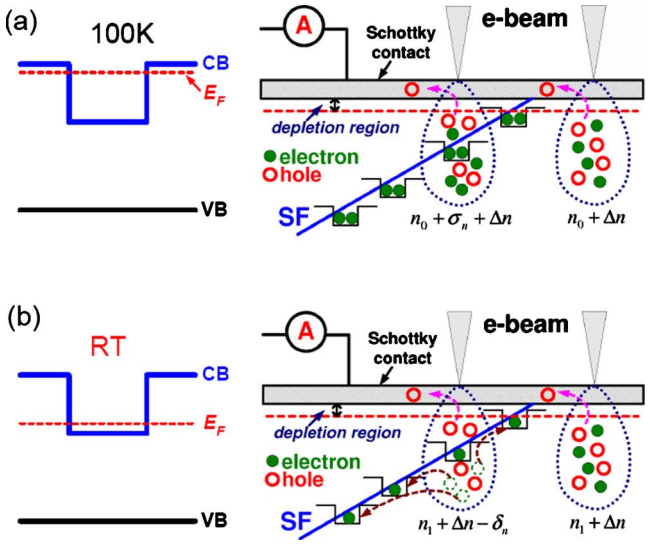

FIG. 5. (Color online) Carrier dynamics regarding the modulation of minority carrier lifetime at the SFs. (a) Explanation of positive EBIC contrast of the SF at 100 K. The high EBIC contrast is due to the pre-existing electrons at the SF which recombine with the holes. (b) Explanation of negative EBIC contrast at RT. The QW pumps out the electrons in the excitation volume, resulting in the reduction of electron density. Owing to the reduction, an increase of the minority carrier lifetime is realized.

No interface roughness is seen, which suggests that the SF has an ideal QW structure. The formation of such a SF is schematically illustrated in Fig. 3(b). It forms by shearing the 4H structure in the $[1\bar{1}00]$ direction during the passage of a PD, which is a Shockley-type SF. Since no external shear stress is used, the driving force for the SF formation is probably due to the recombination-enhanced dislocation glide, where the glide activation energy is supplied from nonradiative recombination at the mobile dislocation core.[17–19]

Detailed EBIC analysis was performed to obtain a understanding of the carrier dynamics inside the ideal QW structure. Figure 4(a) shows the temperature-dependent EBIC contrasts of the SF (rectangular symbol) and PDs (triangular symbol for C-core partial and circular symbol for Si-core partial). The EBIC contrast of the SF decreases with increasing the temperature. It is of interest to stress that after a certain temperature (~250 K), the EBIC contrast of the SF becomes negative and reaches about −5% at RT. To highlight the peculiar contrast, three dimensional EBIC contrast profiles of the SF at 100 K and RT are illustrated in Fig. 4(b). The negative EBIC contrast of the SF means a higher EBIC current than the BG, suggesting that the minority carrier (holes in this case) lifetime increases at the SF region. Such phenomenon is never expected at a defect, since the defects commonly act as the recombination centers. For the case of the PDs,[29] their EBIC contrasts both increase as an increase of the temperature, and then decrease slightly after ~250 K. It indicates that the PDs are accompanied with deep levels in terms of Shockley-Read-Hall statistics.

We thus propose a model to discuss how the ideal QW modulates the minority carrier lifetime, as shown in Fig. 5. The figure is a cross-sectional view of the sample structure with the top Schottky contact collecting carriers. The thin SF lies in the basal plane that is 8° off with respect to the sample surface. It is noteworthy that minority carriers are collected as the signals in the EBIC technique. In the low temperatures, e.g., 100 K [Fig. 5(a)], the Fermi level approaches to the conduction band (CB) of 4H. As a result, the SF-related QW is nearly full of electrons, with the density represented as σ_n. During the e-beam irradiation, a number of electron-hole (e-h) pairs (schematically illustrated in the figure) are generated within an excitation volume (pear-shaped), with the densities of generated electrons and holes being Δn and Δp $(=\Delta n)$, respectively. The radius of the excitation volume is estimated to be ~1.8 μm in 4H-SiC at 20 kV.[30] If the electron density in the matrix is assumed to be n_0, the total electron density in the excitation volume is $n_0+\Delta n$ at the BG, while it becomes $n_0+\sigma_n+\Delta n$ at the SF area. Thus, there exists pretty high probability for minority carriers to be recombined at the SF, resulting in the reduction of minority carrier lifetime (positive EBIC contrast).

When the temperature increases, the Fermi level goes down toward the midgap. Consequently, the number of electrons absorbed at the SF-related QW become less (also evidenced by the temperature-dependent CL intensity), which reduces the recombination probability of the e-h pairs. Especially, at a certain temperature, e.g., RT [Fig. 5(b)], the Fermi level is nearly at the bottom of the QW. In other words, the QW is almost empty. The electrons become relatively easier to be captured by the QW now. In the equilibrium state, the electron density at the SF region is almost the same as that in the matrix (represented as n_1). When the e-beam irradiates the BG, the total electron density is $n_1+\Delta n$ in the excitation volume. At the SF region, however, a certain number of electrons are pumped out from the excitation volume due to the

suction of the nearly empty QW. These electrons diffuse away along the SF plane. Therefore, the total electron density in the excitation volume at the SF region decreases to $n_1+\Delta n-\delta_n$, where δ_n is the electron density diffusing away. Due to the reduction of the electron density, the hole lifetime increases at the SFs (negative EBIC contrast).

Very recently, we notice that Berechman *et al.*[31] observed the bright EBIC contrast also appearing at triangular defects in SiC. The triangular defects can be regarded as another sort of SFs. Therefore, the model proposed above can be also applicable, which suggests that this is a general mechanism for explaining the increase of minority carrier lifetime at the defects. Besides this general mechanism, the experimental results clearly demonstrate that the SFs in SiC functionalize as the ideal QW structure without the interface roughness, whereas the interface roughness commonly exist in the normal QWs owing to the participation of several semiconductors.[32–35]

In summary, we report that the SFs in SiC act as the ideal QW structure for electrons. Due to the "pump effect," an increment of minority carrier lifetime is realized at the SF regions. The dissipation of majority carriers due to the QW nature would serve as a general mechanism regarding the increase of minority carrier lifetime at the defects. Moreover, our result suggests that ideal QW structures can be designed within one semiconductor, which would open the perspective of fabricating the ideal QW structures in other semiconductor systems for various functions.

We thank Canhua Liu and Yongzhao Yao for the helpful discussions. A part of this study was carried out under the NEDO Project supported by METI.

*chen.bin@nims.go.jp

[1] K. V. Ravi, C. J. Varker, and C. E. Volk, J. Electrochem. Soc. **120**, 533 (1973).
[2] B. Shen, R. Zhang, Y. Shi, Y. D. Zheng, T. Sekiguchi, and K. Sumino, Appl. Phys. Lett. **68**, 214 (1996).
[3] A. Qteish, V. Heine, and R. J. Needs, Phys. Rev. B **45**, 6534 (1992).
[4] A. Fissel, Phys. Rep. **379**, 149 (2003).
[5] M. V. S. Chandrashekhar, C. I. Thomas, J. Lu, and M. G. Spencer, Appl. Phys. Lett. **91**, 033503 (2007).
[6] M. H. Hong, A. V. Samant, and P. Pirouz, Philos. Mag. A **80**, 919 (2000).
[7] S. G. Sridhara, F. H. C. Carlsson, J. P. Bergman, and E. Janzen, Appl. Phys. Lett. **79**, 3944 (2001).
[8] Y. Ding, K.-B. Park, J. P. Pelz, K. C. Palle, M. K. Mikhov, B. J. Skromme, H. Meidia, and S. Mahajan, Phys. Rev. B **69**, 041305 (2004).
[9] G. Feng, J. Suda, and T. Kimoto, Appl. Phys. Lett. **92**, 221906 (2008).
[10] G. Feng, J. Suda, and T. Kimoto, Appl. Phys. Lett. **94**, 091910 (2009).
[11] S. I. Maximenko, J. A. Freitas, P. B. Klein, A. Shrivastava, and T. S. Sudarshan, Appl. Phys. Lett. **94**, 092101 (2009).
[12] J. P. Bergman, H. Lendenmann, P. Å. Nilsson, U. Lindefeldt, and P. Skytt, Mater. Sci. Forum **353–356**, 299 (2001).
[13] M. Skowronski and S. Ha, J. Appl. Phys. **99**, 011101 (2006).
[14] B. Chen, T. Sekiguchi, T. Ohyanagi, H. Matsuhata, A. Kinoshita, and H. Okumura, J. Appl. Phys. **106**, 074502 (2009).
[15] R. E. Stahlbush, J. B. Fedison, S. D. Arthur, L. B. Rowland, J. W. Kretchmer, and S. Wang, Mater. Sci. Forum **389-393**, 427 (2002).
[16] W. Si, M. Dudley, H. Kong, J. Sumakeris, and C. Carter, J. Electron. Mater. **26**, 151 (1997).
[17] S. Ha, M. Skowronski, J. J. Sumakeris, M. J. Paisley, and M. K. Das, Phys. Rev. Lett. **92**, 175504 (2004).
[18] A. Galeckas, J. Linnros, and P. Pirouz, Phys. Rev. Lett. **96**, 025502 (2006).
[19] W. R. L. Lambrecht and M. S. Miao, Phys. Rev. B **73**, 155312 (2006).
[20] M. E. Twigg, R. E. Stahlbush, M. Fatemi, S. D. Arthur, J. B. Fedison, J. B. Tucker, and S. Wang, Mater. Sci. Forum **457-460**, 537 (2004).
[21] P. Pirouz, J. L. Demenet, and M. H. Hong, Philos. Mag. A **81**, 1207 (2001).
[22] S. Ha, M. Benamara, M. Skowronski, and H. Lendenmann, Appl. Phys. Lett. **83**, 4957 (2003).
[23] U. Lindefelt, H. Iwata, S. Öberg, and P. R. Briddon, Phys. Rev. B **67**, 155204 (2003).
[24] H. Iwata, U. Lindefelt, S. Öberg, and P. R. Briddon, Phys. Rev. B **65**, 033203 (2001).
[25] M. S. Miao, S. Limpijumnong, and W. R. L. Lambrecht, Appl. Phys. Lett. **79**, 4360 (2001).
[26] T. Sekiguchi and K. Sumino, Rev. Sci. Instrum. **66**, 4277 (1995).
[27] H. Matsuhata, H. Yamaguchi, I. Nagai, T. Ohno, R. Kosugi, and A. Kinoshita, Mater. Sci. Forum **600-603**, 321 (2009).
[28] W. Götz, A. Schoner, G. Pensl, W. Suttrop, W. J. Choyke, R. Stein, and S. Leibenzeder, J. Appl. Phys. **73**, 3332 (1993).
[29] B. Chen, J. Chen, T. Sekiguchi, T. Ohyanagi, H. Matsuhata, A. Kinoshita, H. Okumura, and F. Fabbri, Appl. Phys. Lett. **93**, 033514 (2008).
[30] K. Kanaya and S. Okayama, J. Phys. D **5**, 43 (1972).
[31] R. A. Berechman, M. Skowronski, and Q. Zhang, J. Appl. Phys. **105**, 074513 (2009).
[32] P. G. Neudeck, H. Du, M. Skowronski, D. J. Spry, and A. J. Trunek, J. Phys. D **40**, 6139 (2007).
[33] V. Narayanamurti, Science **235**, 1023 (1987).
[34] S. Nakamura, Science **281**, 956 (1998).
[35] R. G. Mani, J. H. Smet, K. Klitzing, V. Narayanamurti, W. B. Johnson, and V. Umansky, Nature (London) **420**, 646 (2002).